

Impact of chaotic magnetic field on mass-radius relation of rotating neutron stars

Muhammad Lawrence Pattersons¹, Freddy Permana Zen^{1,2}, and Getbogi Hikmawan¹

¹Theoretical High Energy Physics Group, Department of Physics, Institut Teknologi Bandung, Jl. Ganesha 10, Bandung, 40132, Indonesia

²Indonesia Center for Theoretical and Mathematical Physics (ICTMP), Institut Teknologi Bandung, Jl. Ganesha 10, Bandung, 40132, Indonesia

E-mail: m.pattersons@proton.me, fpzen@fi.itb.ac.id, getbogi@fi.itb.ac.id

Abstract. Observations reveal that magnetic fields on neutron stars (NSs) are in the range of 10^{8-15} G. Apart from being celestial bodies, NSs are normally rotating. In this work, we study the impact of a chaotic magnetic field on the mass-radius relation of the rotating NSs. We employ an equation of state of NSs with the nuclei in the crust and hyperons in the core. We use Hartle-Thorne formalism as an approximation of the rotating NSs. For the magnetic field ansatz, we use the one coupled to the energy density. We find that the magnetic field can decrease radius of NS. In contrast, the increment of the magnetic field increases the compactness and deformation of rotating NSs.

1 Introduction

It has been widely understood that the evolution of the massive stars whose mass is $8-25 M_{\odot}$ ended when neutron stars (NSs) formed. The corresponding formation is due to the stars' gravitational collapse during Type-II, Ib, or Ic supernova explosion phenomena [1, 2]. NSs are dense, compact remnants of evolved stars, with degenerate fermions compressed by strong gravitational fields [3]. NSs are normally rotating as all celestial objects tend to naturally always rotate due to the law of angular momentum conservation [4]. Rapidly rotating NSs are observed as pulsars [5].

NSs have a wide range of magnetic fields. Observations indicate that magnetic fields on NSs are at least in the range of 10^{8-15} G. New classes of pulsars such as Anomalous X-ray pulsars (AXPs) and Soft-Gamma Repeater pulsars (SGRs) have been identified producing vast magnetic fields. SGR is associated with remnants of a supernova, which is a young NS [6]. Highly magnetized NSs, i.e. magnetars, are typically slowly spinning NSs whose emission is thought to be powered by the decay of their large ($\geq 10^{12}$ G) magnetic fields [7]. Moreover, observations on some AXPs also indicate that AXPs surface magnetic field is around $10^{14} - 10^{15}$ G [6].

Konno et al. [8] calculated the deformation of NSs resulting from rotation and the presence of magnetic fields. In their analysis, a polytropic equation of state (EOS) was employed. Their findings indicate that for magnetars, the deformation induced by magnetic fields is dominant, whereas for typical pulsars, the magnetic effect is negligible. Mallick & Schramm [9] investigated mass corrections and the deformation of NSs under the influence of magnetic fields, treating the magnetic field as an anisotropy in the energy-momentum tensor (EMT). Interestingly, despite focusing on static NSs, their approach was based on the Hartle-Thorne (HT) formalism [10, 11], which is typically applied to rotating relativistic stars. In their work, magnetic perturbations in static configurations were treated analogously to rotational perturbations, following the HT approximation. They considered both very stiff and very soft EOS models in their study. Lopes & Menezes [12] explored the effects of chaotic magnetic fields on NSs. A key advantage of incorporating a chaotic magnetic field lies in the elimination of anisotropy, simplifying the mathematical formulation. They also introduced an ansatz where the magnetic field is coupled to the

energy density of the NS. For their EOS models, they utilized two variations: one including hyperons and one without. However, the rotation of NSs was not considered in their analysis.

Building on previous studies, we investigate the influence of the chaotic magnetic field on the mass-radius relationship of rotating NSs. The rotational aspects are modeled using the HT formalism, while the magnetic field is described by the Lopes-Menezes ansatz. The EOS employed in this work is based on the realistic model proposed by Miyatsu et al. [13], which includes nuclei in the crust and hyperons in the core. The algorithm of the numerical simulation follows the one used in Refs. [14, 15].

The remainder of this paper is organized as follows. In Section 2, we outline the formulations employed in this study. Section 3 presents the numerical results and a discussion of their implications. Finally, we provide a summary of our findings in Section 4.

2 Mathematical Formulations

To make the discussion self-contained, in Sect. 2.1, we briefly review the chaotic magnetic field of NSs, while the HT formalism is given in Sect. 2.2. It is important to note that in the mathematical formulations we use $G = c = 1$

2.1 Chaotic magnetic field of Neutron Stars

It has been widely understood that the magnetic field could generate anisotropy within NSs [6, 9, 16]. This problem would make the HT formalism for rotational configuration becomes more complex (please see Refs. [1, 17]). For the magnetic field B in the z -direction, it is well-known that the stress tensor is written in the form: $\text{diag}(\frac{B^2}{8\pi}; \frac{B^2}{8\pi}; -\frac{B^2}{8\pi})$, being non identical [12]. In Ref. [18], it is argued that the effect of a magnetic field can be described using the concept of pressure only in the case of a small-scale chaotic field. Under this condition, the pressure due to the magnetic field p_B is shown to be consistent with field theory. Authors in Ref. [12] agreed to this argument. Now p_B reads

$$p_B = \frac{1}{3} \langle T_j^j \rangle = \frac{1}{3} \left(\frac{B^2}{8\pi} + \frac{B^2}{8\pi} - \frac{B^2}{8\pi} \right) = \frac{B^2}{24\pi}, \quad (1)$$

where T_j^j denotes the spatial components of the EMT. With this formulation in our hand, we can avoid the anisotropy which is caused by the appearance of magnetic field. The total energy density ϵ and total pressure p now write

$$\epsilon = \epsilon_m + \frac{B^2}{8\pi}, \quad (2)$$

$$p = p_m + \frac{B^2}{24\pi}, \quad (3)$$

where the subscript m stands for the matter contribution.

An ansatz of the magnetic field is proposed in Ref. [12], i.e.

$$B = B_0 \left(\frac{\epsilon_m}{\epsilon_0} \right)^\gamma + B_{surf}. \quad (4)$$

Here B_0 can be interpreted as the magnetic field at the center of the star, ϵ_0 is the energy density at the center of the NS with maximum mass when the magnetic field is zero, γ is any positive number (in this work we use $\gamma = 10^{-3}$)¹, and B_{surf} is the magnetic field at the surface of the NSs.

2.2 Hartle-Thorne Formalism for Rotating Relativistic Stars

In HT formalism, the metric reads [1, 10, 11, 15]

$$ds^2 = -e^{2\nu} dt^2 + e^{2\lambda} dr^2 + r^2 e^{2\psi} (d\phi - \omega dt)^2 + r^2 e^{2\mu} d\theta^2, \quad (5)$$

where ω is the angular velocity of the local inertial frame, which is proportional to the star's angular velocity Ω relative to a distant observer. In this case, ω and Ω satisfy $\omega = \Omega - \bar{\omega}$, where $\bar{\omega}$ is the angular velocity of the star relative to the local inertial frame.

Due to rotational perturbation, the exponential functions in Eq. (5) are expanded as the following:

$$e^{2\nu} = e^{2\varphi} [1 + 2(h_0 + h_2 P_2(\cos \theta))], \quad (6)$$

¹Values of γ around 10^{-3} yield similar results, while setting γ to much larger values (e.g., 1, 2, 3) significantly affects the outcome, likely due to changes in energy density affecting the core-crust transition.

$$e^{2\lambda} = \left[1 + \frac{2}{r} (m_0 + m_2 P_2(\cos \theta)) \left(1 - \frac{2m(r)}{r} \right)^{-1} \right] \left(1 - \frac{2m(r)}{r} \right)^{-1} \quad (7)$$

$$e^{2\psi} = r^2 \sin^2 \theta [1 + 2(v_2 - h_2)P_2(\cos \theta)], \quad (8)$$

$$e^{2\mu} = r^2 [1 + 2(v_2 - h_2)P_2(\cos \theta)]. \quad (9)$$

Here h_0 , h_2 , m_0 , m_2 , and v_2 are functions of perturbation due to rotation; $P_2(\cos \theta)$ is the second order of Legendre polynomial; $e^{2\varphi}$ is a function which is constrained by

$$\frac{d\varphi}{dr} = \frac{m + 4\pi r^3 p}{r(r - 2m)}, \quad (10)$$

where m is the mass function which is constrained by

$$\frac{dm}{dr} = 4\pi r^2 \epsilon. \quad (11)$$

The equilibrium equation of the relativistic bodies is given by the Tolman-Oppenheimer-Volkoff (TOV) equation [1, 10, 19], i.e.

$$\frac{dp}{dr} = -(\epsilon + p) \frac{d\varphi}{dr}. \quad (12)$$

For a rotating configuration, $\bar{\omega}$ can be calculated by solving the following equation [10]:

$$\frac{1}{r^4} \frac{d}{dr} \left(r^4 j \frac{d\bar{\omega}}{dr} \right) + \frac{4}{r} \frac{dj}{dr} = 0, \quad (13)$$

where

$$j = e^{-\varphi} \left(1 - \frac{2m}{r} \right)^{1/2}. \quad (14)$$

The boundary condition at $r = 0$ is $\bar{\omega} = \omega_c$, where ω_c can be chosen arbitrarily.

It is important to note that Eq. (10), Eq. (11), and Eq. (12) deal with static configuration. Moreover, due to the rotation, the radius of the star is deformed. To obtain the mass and radius corrections of the rotating NS, we have to employ Einstein field equation

$$R_\nu^\mu - \frac{1}{2} \mathcal{R} \delta_\nu^\mu = 8\pi T_\nu^\mu, \quad (15)$$

where R_ν^μ is Ricci tensor, \mathcal{R} is Ricci scalar, δ_ν^μ is Kronecker delta, and T_ν^μ denotes the EMT.

By calculating the Einstein field equation, for the (tt) -component of the $l = 0$ order, we can obtain

$$\frac{dm_0}{dr} = 4\pi r^2 \frac{d\epsilon}{dp} (\epsilon + p) \mathcal{P}_0 + \frac{1}{12} j^2 r^4 \left(\frac{d\bar{\omega}}{dr} \right)^2 - \frac{1}{3} r^3 \left(\frac{dj}{dr} \right)^2 \bar{\omega}^2. \quad (16)$$

From the (rr) -component of the $l = 0$ order, we can obtain

$$\frac{d\mathcal{P}_0}{dr} = -\frac{m_0 (1 + 8\pi r^2 p)}{(r - 2m)^2} - \frac{8\pi r^2 (\epsilon + p)}{2(r - 2m)} \mathcal{P}_0 + \frac{1}{12} \frac{r^4 j^2}{r - 2m} \left(\frac{d\bar{\omega}}{dr} \right)^2 + \frac{1}{3} \left[\frac{d}{dr} \left(\frac{r^3 j^2 \bar{\omega}^2}{r - 2m} \right) \right]. \quad (17)$$

Here \mathcal{P}_0 is originally the 0th-order of expansion of pressure perturbation factor $\mathcal{P} = \mathcal{P}_0 + \mathcal{P}_2 P_2(\cos \theta)$. The boundary conditions at $r = 0$ are $m_0(0) = 0$ and $\mathcal{P}_0(0) = 0$.

Mass correction δM of the star is given by

$$\delta M = m_0(R) + \frac{L^2}{R^3}, \quad (18)$$

where R denotes the radius of the star, and L denotes the angular momentum, which satisfies

$$L = \frac{R^3}{2} (\Omega - \bar{\omega}(R)). \quad (19)$$

Thus, the total mass reads

$$M = M_{STAT} + \delta M, \quad (20)$$

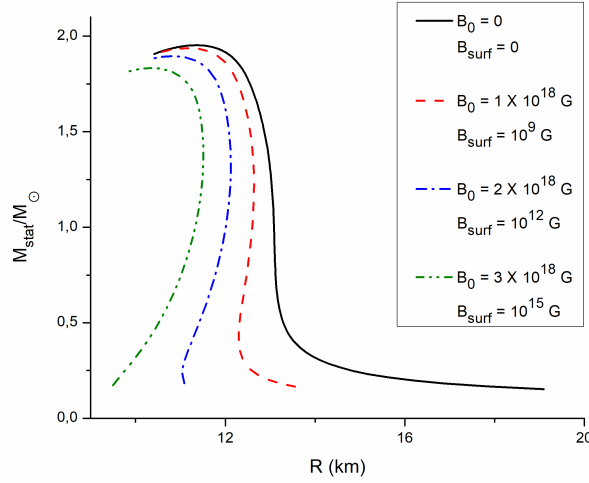


Figure 1: Impact of chaotic magnetic field on mass-radius relation of NSs for static configuration.

where M_{STAT} is the mass of NSs within static configuration which is obtained by solving Eq. (10), Eq. (11), and Eq. (12) simultaneously.

From the $(\theta\theta)$, $(\phi\phi)$, (θr) , and (rr) components of the $l = 2$ order of Einstein field equation, we obtain

$$\frac{dv_2}{dr} = -2 \frac{d\varphi}{dr} h_2 + \left(\frac{1}{r} + \frac{d\varphi}{dr} \right) \left[-\frac{1}{3} r^3 \frac{dj^2}{dr} \bar{\omega}^2 + \frac{1}{6} j^2 r^4 \left(\frac{d\bar{\omega}}{dr} \right)^2 \right], \quad (21)$$

$$\begin{aligned} \frac{dh_2}{dr} = & -2 \frac{d\varphi}{dr} h_2 + \frac{[8\pi r(\epsilon + p) - \frac{4m}{r^2}]}{(r - 2m) \left(2 \frac{d\varphi}{dr} \right)} h_2 - \frac{4v_2}{r(r - 2m) \left(2 \frac{d\varphi}{dr} \right)} \\ & + \frac{r^3 j^2}{6} \left[\frac{d\varphi}{dr} r - \frac{1}{(r - 2m) \left(2 \frac{d\varphi}{dr} \right)} \right] \left(\frac{d\bar{\omega}}{dr} \right)^2 \\ & - \frac{r^2 \bar{\omega}^2}{3} \left[\frac{d\varphi}{dr} + \frac{1}{(r - 2m) \left(2 \frac{d\varphi}{dr} \right)} \right] \frac{dj^2}{dr}. \end{aligned} \quad (22)$$

The boundary conditions at $r = 0$ are $v_2(0) = 0$ and $h_2 = 0$.

There exists a formula [1, 10]

$$\mathcal{P}_2 = -h_2 - \frac{1}{3} r^2 e^{-2\varphi} \bar{\omega}^2. \quad (23)$$

The radius correction of the star is given by

$$\delta r = \xi_0(R) + \xi_2(R) P_2(\cos \theta), \quad (24)$$

where

$$\begin{aligned} \xi_0 &= -\mathcal{P}_0(\epsilon + p) \left(\frac{dp}{dr} \right)^{-1}, \\ \xi_2 &= -\mathcal{P}_2(\epsilon + p) \left(\frac{dp}{dr} \right)^{-1}. \end{aligned} \quad (25)$$

Finally, we can calculate the radius of the pole R_{POL} and the radius of the equator R_{EQ} [1, 20]

$$R_{POL} = R + \xi_0 + \xi_2, \quad (26)$$

$$R_{EQ} = R + \xi_0 - \frac{\xi_2}{2}. \quad (27)$$

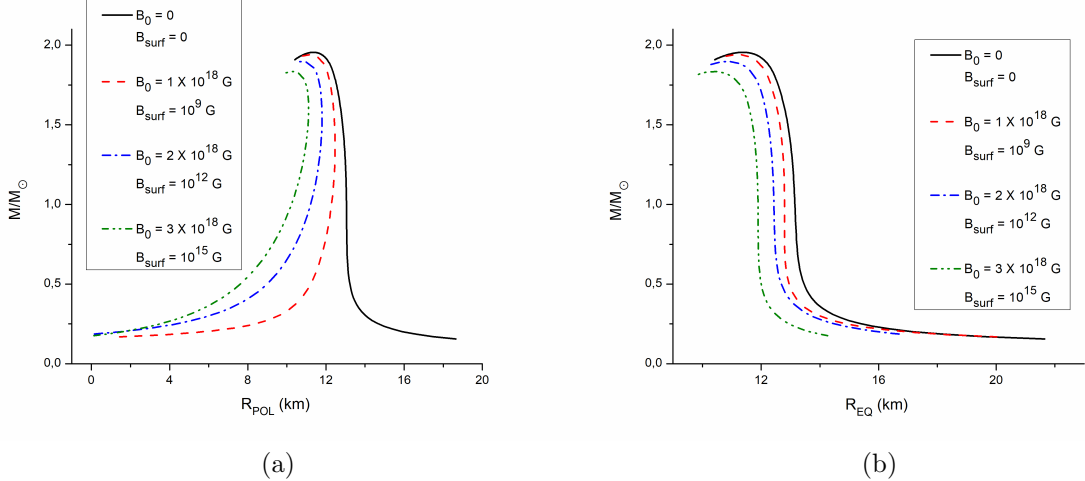


Figure 2: Impact of chaotic magnetic field on mass-radius relation of NSs for (a) polar radius, and (b) equatorial radius.

3 Results and Discussion

We numerically solved all differential equations using Euler method. For the value of Ω , we use $\Omega = 1000 \text{ s}^{-1}$. For the initial value of $\bar{\omega}$ (i.e. ω_c), we choose 240 s^{-1} in this work. Please note that this value is much less than the value used in Ref. [21], i.e. $\bar{\omega} = 3000 \text{ s}^{-1}$. Moreover, our initial value of ω_c is more suitable for HT formalism. It is worth noting that $\bar{\omega}(r)$ increases as r increases. On the other side, we have an insight that according to Ref. [22], the HT formalism is accurate to better than 1 per cent even for the fastest millisecond pulsars. However, putting $\bar{\omega}_c = 3000 \text{ s}^{-1}$ in the calculation is still potential to be dangerous, for the HT formalism is basically an approximation for slowly rotating relativistic stars. So our value of $\bar{\omega}_c$ is safer than the one in Ref. [21]. If we compare our initial value of $\bar{\omega}$ to the ones of Ref. [1] and Ref. [14] which chose $\bar{\omega}_c = 0$, our choice of $\bar{\omega}_c$ is more realistic for general rotating NS, since their choice seems to only agree the NSs with very slow rotation. The same value of ω_c and same reasoning of the choice have been highlighted by authors in Ref. [15].

Fig. 1 presents the mass-radius relationship of NSs in a static configuration. The presence of a chaotic magnetic field reduces the radius of NSs, as indicated by the leftward shift of the curves with increasing magnetic field strength, suggesting that a chaotic magnetic field contributes to greater compactness of the stars. Compactness, defined as the mass-to-radius ratio, is directly influenced by this field. Notably, the radius reduction is pronounced in the case where $B_0 = 3 \times 10^{18} \text{ G}$ and $B_{\text{surf}} = 10^{15} \text{ G}$, indicating that the radius decrease is non-linear with respect to the increase in the chaotic magnetic field. However, our results diverge from those reported by the authors in Ref. [12], where the chaotic magnetic field was found to increase the radius of NSs. This discrepancy may be attributed to the different EOS employed in their study. Furthermore, it is worth noting that as the magnetic field strength increases, the mass-radius curve begins to resemble that of quark stars. For more detailed discussions on quark stars, please refer to Refs. [23, 24, 25].

Fig. 2 shows the polar and equatorial radii, indicating the deformation of rotating NSs. The deformation is less pronounced for the NSs with higher masses but becomes more evident for lower masses. This can be seen in the mass-radius relations of magnetized rotating NSs, where the curves in panel (a) and panel (b) diverge significantly at lower mass values. A comparison with Fig. 3 which depicts rotating NSs without a magnetic field, reveals that deformation still occurs but with only a slight difference between the polar and equatorial radii. This deformation due to rotation is expected and is similar to the Earth's rotational deformation, where the polar radius is smaller than the equatorial radius [1]. The key takeaway from Fig. 2 and Fig. 3 is that the deformation induced by the magnetic field is much more significant than that caused by rotation.

Additionally, Fig. 2 demonstrates a substantial increase in deformation with increasing magnetic field strength. This contrasts with the findings in Ref. [16], where NSs were also deformed by the presence of a magnetic field, but the increase in deformation with increasing field strength was less pronounced, leading to nearly coincident curves. This difference may stem from differences in the ansatz and core EOS employed in their model.

We present 3- and 2-dimensional illustrations of the NSs in Fig. 4. We take examples from the case of $B_0 = 3 \times 10^{18} \text{ G}$ and $B_{\text{surf}} = 10^{15} \text{ G}$. At lower mass, the star's shape becomes very oblate. At $M = 0.31 M_{\odot}$, $R_p = 4.96 \text{ km}$, and $R_e = 12.51 \text{ km}$; at $M = 0.51 M_{\odot}$, $R_p = 7.75 \text{ km}$, and $R_e = 11.99 \text{ km}$; $M = 1.18 M_{\odot}$, $R_p = 10.67 \text{ km}$, and $R_e = 11.87 \text{ km}$; and $M = 1.83 M_{\odot}$, $R_p = 10.48 \text{ km}$, and R_e

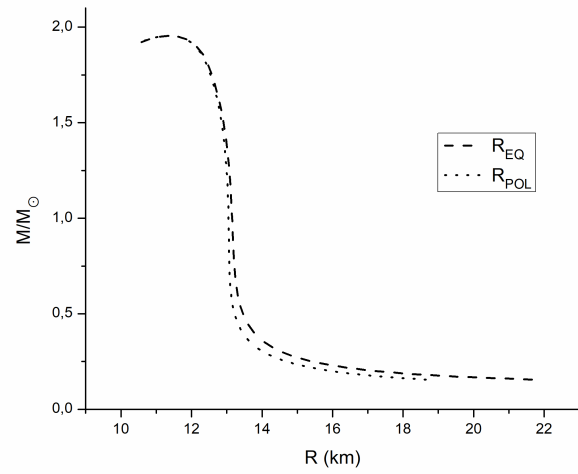


Figure 3: Mass-radius relation of the deformed NSs without magnetic field

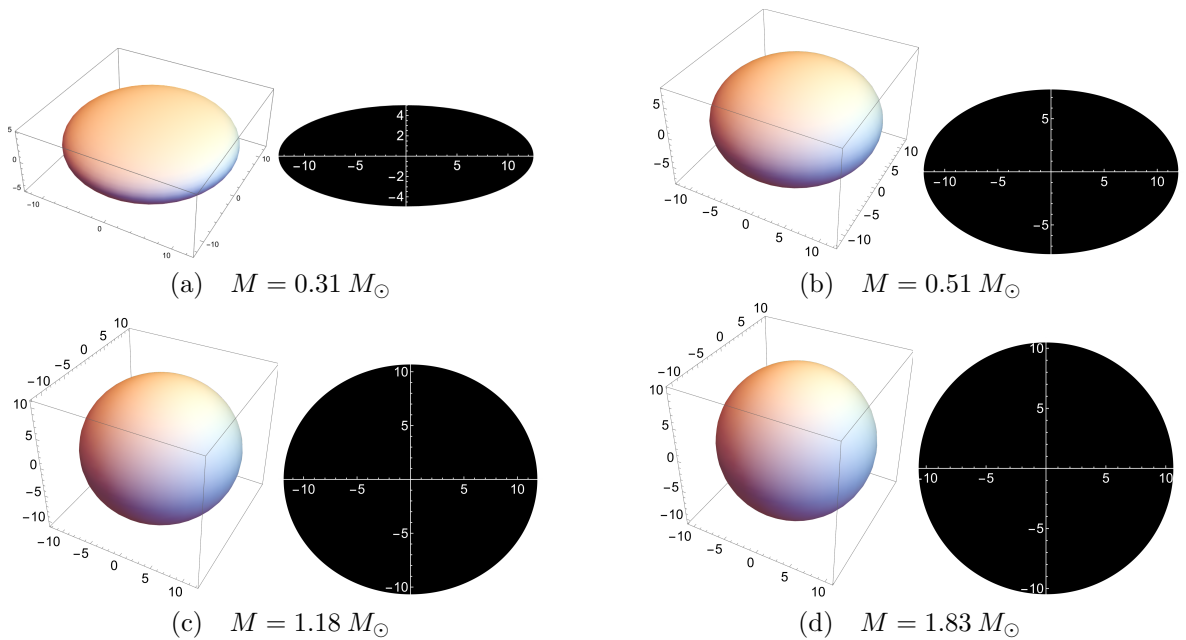


Figure 4: Illustrations of 3- and 2-dimensional deformation of neutron stars in each particular mass at $B_0 = 3 \times 10^{18}$ G and $B_{surf} = 1 \times 10^{15}$ G.

$= 10.63$ km. It is noteworthy to compare our results with those presented in Ref. [1]. The deformation of rotating NSs in our study is significantly more pronounced than in their findings, which are based on rotating NSs with anisotropic pressure of matter, but without considering the contribution of a magnetic field to the deformation. This fact strengthens our argument that the magnetic field strongly induces the deformation of rotating NSs.

4 Conclusion

In this study, we calculated the mass and radius of NSs under the influence of a chaotic magnetic field, enabling us to obtain the mass-radius relationship for these stars. Our findings indicate that the magnetic field decreases the radius of NSs. Additionally, while the chaotic magnetic field contributes to a reduction in radius, it simultaneously enhances the compactness and deformation of rotating NSs, with significant deformation occurs at lower mass values.

Acknowledgements

MLP acknowledges the Indonesia Endowment Fund for Education Agency (LPDP) for financial support. Special thanks are extended to Anna Campoy Ordaz for making her code publicly available, which allowed MLP to modify it for use in this work. FPZ and GH would like to thank Kemendikbudristek Republic of Indonesia (through LPPM ITB, Indonesia) for partially financial support.

References

- [1] Pattersons M L and Sulaksono A, 2021, *Eur. Phys. J. C*, **81**, 698
- [2] Vidaña I, 2018, *Eur. Phys. J. Plus*, **133**, 445
- [3] Reisenegger A, 2001, *ASP Conf. Ser.*, **248**, 469–478
- [4] Sivaram C and Arun K, 2012, *Open Astron. J.*, **5**, 7–11
- [5] Yasrina A and Pramono N A, 2020, *J. Technomaterial Phys.*, **02**, 02
- [6] Rizaldy A and Sulaksono S, 2018, *J. Phys. Conf. Ser.*, **1011**, 012083
- [7] Desvignes G, Weltevrede P, Gao Y, Jones D I, Kramer M, Caleb M, Karuppusamy R, Levin L, Liu K, Lyne A G, Shao L, Stappers B and Pétri J, 2024, *Nature Astron.*, **8**, 617–627
- [8] Konno K, Obata T and Kojima Y, 2000, *Astron. Astrophys.*, **356**, 234–237
- [9] Mallick R and Schramm S, 2014, *Phys. Rev. C*, **89**, 045805
- [10] Hartle J B, 1967, *Astrophys. J.*, **150**, 1005–1029
- [11] Hartle J B and Thorne K S, 1968, *Astrophys. J.*, **153**, 807–834
- [12] Lopes L and Menezes D, 2015, *J. Cosmol. Astropart. Phys.*, **2015**, 002
- [13] Miyatsu T, Yamamoto S and Nakazato K, 2013, *Astrophys. J.*, **777**, 1
- [14] Ordaz A C, 2019, Master's Thesis, Universitat de Barcelona
- [15] Pattersons M L, Zen F P, Prihadi H L and Sakti M F A R, 2024, ArXiv, 2404.01837
- [16] Rizaldy R and Sulaksono A, 2018, *J. Phys. Conf. Ser.*, **1080**, 012031
- [17] Beltracchi P and Posada C, 2024, *Phys. Rev. D*, **110**, 024052
- [18] Zel'dovich Y B and Novikov I D, 1971, Introduction to Part II, Stars and Relativity, Dover Publications, 158
- [19] Oppenheimer J R and Volkoff G M, 1939, *Phys. Rev.*, **55**, 374
- [20] Lopes L L, 2024, *Astrophys. J.*, **966**, 184
- [21] Wen D H, Chen W and Liu L G, 2005, *Chin. Phys. Lett.*, **22**, 1604
- [22] Berti E, White F, Maniopoulou A and Bruni M, 2005, *Mon. Not. R. Astron. Soc.*, **358**, 923–938
- [23] Lai X Y and Xu R X, 2009, *Mon. Not. R. Astron. Soc.*, **398**, L31–L35
- [24] Chu P C, Zhou Y, Jiang Y Y, Ma H Y, Liu H, Zhang X M and Li X H, 2021, *Eur. Phys. J. C*, **81**, 93
- [25] Li A, 2022, *EPJ Web Conf.*, **260**, 04001